

ORIENTATIONAL ORDERING OF PROTEIN MICRO- AND NANOPARTICLES IN A NONUNIFORM MAGNETIC FIELD

I.G. Lyakhov^a, T.D. Schneider^b, G.A. Lyakhov^c, and N.V. Suyazov^c

^a Basic Research Program, SAIC-Frederick, Inc, Laboratory of Experimental and Computational Biology, NCI-FCRDC, Frederick, MD 21702, USA.

^b Laboratory of Experimental and Computational Biology, NCI-Frederick, Frederick, MD 21702, USA

^c Wave Research Center, General Physics Institute, Russian Academy of Science, Moscow 119942, Russia (e-mail: lyakhga@orc.ru)

We propose and describe a mechanism of orientational ordering of molecules and multimolecular particles that have incorporated Fe ions. The ordering is provided by a spatially nonuniform magnetic field and by nonuniform distribution of ions in a molecule. Orientational distributions of particles have been calculated for this mechanism. These distributions have been applied to estimate the degree of orientational ordering in suspensions of biological nano- and micromolecules, as well as the times of formation of the ordered state in a magnetic field and the ordered state disturbance as the field is turned off. The estimates have allowed us to contemplate bioparticle types likely to implement the effect.

1. Introduction

The study of the magnetic properties of biological microobjects is one of the promising divisions of biophysics (see, for example, [1]). A number of impressive results were obtained in this field (see [2]), for example, the diamagnetic-to-paramagnetic phase transition in an oxy-Hb-O solution within erythrocytes at a temperature of about 42°C [3]. The magnetic measurement methods developed to date are mostly applicable to proteins that bind metal ions such as Fe(2+), Fe(3+), Co(2+), and Ni(2+). Only these proteins have response to an external magnetic field.

The possibility of artificial saturation of a protein molecule with a large number of Fe ions offers new prospects. Iron ions have an intrinsic magnetic moment oriented along the external field. A material saturated by Fe ions is magnetized and exhibits paramagnetic or even ferromagnetic properties, depending on the volume density of incorporated ions. The magnetic interaction of components of these bio-objects is nontrivial [4].

We consider it reasonable to examine the magnetic properties of Fe-saturated protein molecules (and larger bioparticles) for their spatial orientation in a magnetic field.

To get a lower estimate of the molecule orientation effect, we can neglect the rigidity of the bonds of the Fe-ion electron orbits with the surroundings. In this approximation, the rotating mechanical moment having an effect on bioparticles in a uniform field is zero, since the field-induced bioparticle magnetic moment is parallel to the external magnetic field vector.

In a nonuniform magnetic field, the force acting on a magnetized particle is proportional to the field gradient. This force brings the molecule into translational motion. This motion causes a hydrodynamic resistance force (friction) acting on the bioparticle from the surrounding liquid (water). In the case of a nonuniform distribution of Fe ions in the bioparticle, the application points of these two forces do

not coincide. As a result, a mechanical moment of forces arises, rotating the molecule. Thus, bioparticles can be oriented in a nonuniform magnetic field even in the absence of finite rigidity of the bond between the atomic magnetic moment and the surroundings. Hence, the nonuniformities of the magnetic field and the distribution of Fe ions in the bioparticle are the necessary conditions for the exhibition of the orientation mechanism described below.

We estimated the efficiency of this mechanism of iron containing bioparticle orientation for both separate protein molecules (with sizes of about 10 nm) and larger (micrometer) bioparticles.

2. Interaction between a Fe-ion-containing bioparticle and a nonuniform magnetic field

2.1. A Magnetic field \mathbf{H} acts on an iron containing bioparticle with a force (see [5])

$$\mathbf{F}_m = (\mathbf{m} \nabla) \mathbf{H},$$

where ∇ is the gradient over the observational point coordinates and \mathbf{m} is the induced magnetic moment of the bioparticle; parentheses mean the scalar product of vectors. The center of the region populated by Fe ions may be considered the application point of this force.

We calculate the magnetic moment of a particle with incorporated Fe ions using a model of paramagnetism of free ions. In the unexcited quantum state, the ions are characterized by nonzero angular momentum and magnetic moments of electron shells, caused by the momentum. With no external field, these moments are randomly oriented. As the magnetic field is turned on, the medium magnetization is controlled by the competition of two effects: Fe-ion magnetic moments are oriented along the field, while the perturbations caused by thermal motion tend to restore the uniform distribution of the moment orientations. The total magnetic moment \mathbf{m} of an ion ensemble is aligned along the external field. In the case of not too strong fields and not too low temperatures,

$$\frac{G\mu_B |\mathbf{H}|}{kT} \ll 1,$$

\mathbf{m} is proportional to the external magnetic field \mathbf{H} ,

$$\mathbf{m} = \frac{NG^2 \mu_B^2 \mathbf{H}}{3kT},$$

where N is the number of Fe ions, $\mu_B = 0.93 \cdot 10^{-20} \text{Gs}\cdot\text{cm}^3$ is the Bohr magneton, k is the Boltzmann constant, and T is the Kelvin temperature. The coefficient G is defined by the orbital and spin quantum numbers of the ground state [6]. In metal complexes, where the orbital moment is much smaller than the spin moment, the coefficient G is approximately given by

$$G = \sqrt{n(n+2)},$$

where n is the number of unbound electrons per ion. An analysis of the data [7] for iron ions in various compounds yields the value G from 4.7 to 6, which agrees with Eq.(4) (when $n = 4$ or 5) to the accuracy appropriate for estimates. Hereafter we use the average value of data [7], $G = 5.6$. We note that condition Eq.(3) of the magnetization linearity is obviously met at the reasonable values $H \leq 10^4 \text{Oe}$, $T \geq 300 \text{K}$.

The model yields a lower estimate of the orientation degree of iron containing molecules since it neglects two effects which can increase the orientation degree. First, we neglect stresses in the molecule interatomic bonds, arising as the Fe-ion magnetic moment is turned (that is, electron orbits are turned) in the external magnetic field. In other words, we neglect that the ion magnetic moment has a nonzero rigidity of the bond with the protein molecule. Typically, the Fe ion is bound with its neighbors by four interatomic bonds. The turning of the Fe-ion electron orbits should induce an additional moment turning the whole molecule in a required direction even in a uniform magnetic field. To estimate the rigidity of the bond of the Fe-ion magnetic moment with the biomolecule, one should comparatively study the NMR spectra of iron incorporations in the protein molecule and the spectra of free iron atoms. This study would be an experimental method for estimating the bonding energy.

Second, we neglect the interaction between the magnetic moments of Fe ions, supposing that they are exposed to the external field only. Hence, the induced magnetic moment of the whole region of incorporated ions is equal to a simple sum of the moments induced by the external field in separate ions. In a close arrangement of Fe ions, this interaction strengthens the magnetization of the particle. If the distance between Fe ions is shortened to several ion radii, an ion ensemble becomes a typical ferromagnet and the induced magnetic moment of the medium increases many times in comparison with the paramagnetic medium. In the intermediate case of moderate interatomic spacings, partial manifestation of ferromagnetism can be approximately taken into account after substitution of the coefficient G in Eq. (3) with $G_{\text{eff}} > G$. Determination of G_{eff} for the region of ion incorporations in protein molecules is to be a subject of further expected studies to refine these estimates. For now we can just argue that the actual orientation degree of protein molecules and iron containing particles should exceed the estimate given above.

The substitution of Eq.(3) into Eq.(1) using the equation $[\nabla \times \mathbf{H}] = 0$ yields the magnetic force

$$\mathbf{F}_m = \frac{4\pi N G^2 \mu_B^2}{3kT} \cdot \nabla w,$$

where the energy density of the magnetic field is given by

$$w = \frac{H^2}{8\pi}.$$

2.2. The necessity of high nonuniformity of the magnetic field for efficient turning of iron containing particles imposes strict requirements upon the experimental conditions. These requirements are met, for example, by the field induced near a thin ferromagnetic wire (with the radius $a \sim 10^{-2} - 10^{-4}$ cm) transversely magnetized by the uniform magnetic field \mathbf{H}_0 . In this case, even moderate fields (several hundred Oersteds) magnetize the ferromagnetic wire up to saturation [5] and induce a magnetization vector \mathbf{M}_s (the magnetic moment of microcurrents per unit volume of the medium [5]) whose direction coincides with that of the vector \mathbf{H}_0 . The magnetization value M_s reaches about 2000Gs (1700Gs for iron [8]). A ferromagnetic wire magnetized in such a way induces a secondary highly inhomogeneous nonuniform field \mathbf{H}_s around itself. This field can exceed the uniform magnetizing field H_0 near the wire by dozens of times (see Eq.(8) below). We propose to employ the wire secondary field for orientating protein particles along the axis normal to the wire. This axis is parallel to vectors \mathbf{M}_s and \mathbf{H}_0 .

We introduce a Cartesian frame of reference with the x axis directed along \mathbf{H}_0 ; axis z is directed along the wire axis (see Fig.1). The nonuniform magnetic field induced by the wire can be written via the integral over its cylindrical surface S ,

$$\mathbf{H}_s(\mathbf{R}) = \iint_S (\mathbf{M}_s \mathbf{n}) \frac{(\mathbf{R} - \mathbf{R}_s)}{|\mathbf{R} - \mathbf{R}_s|^3} dS,$$

where \mathbf{R} and \mathbf{R}_s are the vectors from the coordinate origin to the observation point and to the cylinder (wire) surface, and \mathbf{n} is the unit vector of the normal to this surface. The integration yields the components of the wire magnetic field vector,

$$\mathbf{H}_s = \frac{2\pi M_s a^2}{r^2} \begin{Bmatrix} \cos 2\psi \\ \sin 2\psi \\ 0 \end{Bmatrix},$$

where r and ψ are the polar coordinates in the xy plane. We note that the direction of the wire magnetic field does not coincide with that of the polar vector $\mathbf{r} = \{x, y, 0\}$, except for the points on the axis x .

The magnetic field acting on a particle is given by

$$\mathbf{H} = \mathbf{H}_s + \mathbf{H}_0.$$

Near the wire, where the field H_0 can be neglected in comparison with the wire field H_s (under the experimental conditions considered above: an iron wire at $H_0 \sim 300$ Oe), magnetic force Eq.(5) is directed to the wire axis,

$$\mathbf{F}_m \approx - \frac{8\pi^2 N (G\mu_B M_s)^2 a^4}{3kTr^5} \begin{Bmatrix} \cos \psi \\ \sin \psi \\ 0 \end{Bmatrix}.$$

3. Time for a bioparticle to turn and the optimum configuration of magnetic incorporations

3.1. In addition to the magnetic force, the bioparticle is subject to hydrodynamic resistance forces caused by the surrounding liquid. Protein molecule sizes are of the order of $l_p \sim 10^{-6}$ cm, while the size of large bioparticles considered here is $l_p \sim 10^{-4} - 10^{-3}$ cm. At these both scales, the Reynolds number $Re = 2\rho v l_p / \eta$ (ρ and η are the water density and dynamic viscosity and v is the characteristic velocity of motion) is much less than unity. Therefore, the resistance forces of the surrounding liquid can be considered to be proportional to the particle velocity [9]. At these scales, we can also neglect inertial effects. Thus, the problem is reduced to a quasi-static one (time is only a parameter), and the molecule motion equations are transformed into the equilibrium conditions of a solid. These conditions allow the unique determination of the velocities of the bioparticle translational and rotational motions depending on its position and orientation. The motion mode is almost instantly established in a time of the order $\rho l_p^2 / 3\eta \sim 10^{-5} - 10^{-11}$ s [9]. Here we neglect the diffusion effects caused by

thermal motion of the liquid molecules surrounding the particle. These effects will be taken into account below in the calculation of the orientational distribution of particles.

To estimate the time of the turn of an iron containing bioparticle in a magnetic field and the influence of a nonuniform arrangement of incorporations, we consider the simplest model of two rigidly joined spheres (see Fig.2). One sphere with radius r_1 is uniformly filled with Fe ions and uniformly magnetized. Another sphere with radius r_2 contains no incorporations and is not magnetized. Magnetic force Eq.(5) acts on the former sphere, being applied to the sphere center. As an estimation, we suppose that the mechanical forces and the liquid resistance moments may be calculated separately for either sphere. The hydrodynamic resistance forces are distributed over the sphere surface. We also suppose that the total action of liquid may be reduced to the Stokes force (resistance force of translational motion) applied to the sphere center,

$$\mathbf{F}_{1,2} = -6\pi r_{1,2} \eta \mathbf{v}_{1,2},$$

where $\mathbf{v}_{1,2}$ is the motion velocity of the center, as well as to the mechanical moment of rotation resistance,

$$\mathbf{K}\boldsymbol{\omega}_2 = -8\pi \eta r_{1,2}^3 \boldsymbol{\omega}_2,$$

where $\boldsymbol{\omega}$ is the rotation angular velocity [9].

To make things simpler, we suppose that the particle axis (that is, the vector \mathbf{r}_{21} from the second sphere center to the first sphere center) lies in the plane normal to the wire (axis z), hence the particle makes plane-parallel motion in this plane. The particle coordinates meet the condition $y/x \ll 1$. The motion equation is reduced to the bioparticle equilibrium condition, that is, to two equal-zero components of the resulting force,

$$\mathbf{F}_m + \mathbf{F}_1 + \mathbf{F}_2 = 0,$$

and the total mechanical moment, which, apart from Eq.(12), also incorporate moments of forces Eq. (5) and Eq.(11). As an axis of moment reference, we take the axis parallel to the wire, passing through the second sphere center. Then the equation of moments is written as

$$\left[\mathbf{r}_{21} \times (\mathbf{F}_m + \mathbf{F}_1) \right] + \mathbf{K}_1 + \mathbf{K}_2 = 0,$$

where the brackets mean the vector product. Equilibrium conditions Eq.(13) and Eq.(14) in the components yield

$$\begin{aligned} F_m + 6\pi\eta (r_2 + r_1) \left[r_1 \sin\theta \frac{d\theta}{dt} - v_x \right] &= 0, \\ -6\pi\eta (r_2 + r_1) \left[r_1 \cos\theta \frac{d\theta}{dt} + v_y \right] &= 0, \\ -(r_2 + r_1) \left[F_m \sin\theta + 2\pi\eta \left((7r_1^2 - r_1r_2 + 4r_2^2) \frac{d\theta}{dt} - 3r_1 v_x \sin\theta + 3r_1 v_y \cos\theta \right) \right] &= 0, \end{aligned}$$

where θ is the angle between the particle axis and the vector \mathbf{H} (axis x in Fig.2), $v_{x,y}$ are the velocity components of the second sphere center. Eliminating the velocities $v_{x,y}$ from Eq.(15), we arrive at the differential equation for the bioparticle orientation angle,

$$\frac{d\theta}{dt} = - \frac{r_2 F_m \sin\theta}{2\pi\eta (r_1 + r_2) (4r_1^2 - r_1 r_2 + 4r_2^2)}.$$

The magnetic force F_m in the layout of Fig.1 is given by

$$F_m = - \frac{4\pi N G^2 \mu_B^2 a^2 M_s (2\pi M_s a^2 + H_0 x^2)}{3kT x^5}.$$

Further we suppose that the value of x/a varies insignificantly within the time of particle rotation. This supposition is substantiated by the fact that the ratio of the times of particle rotation τ_r and particle incidence on the wire τ_f is defined by the ratio of the corresponding motion scales, $\tau_r / \tau_f \sim l_p / x$. A more accurate estimate can be found from Eq.(15). If $r_1 \ll r_2$ and $H_0 / M_s \ll \pi$ (this is exactly the field-to-magnetization ratio which may be advantageously employed in an experiment), the ratio of times is estimated as

$$\frac{\tau_r}{\tau_f} \approx 25 \frac{r_2 x^5}{x^6 - a^6}.$$

Hence, the condition $\tau_r / \tau_f \ll 1$ is met if the particle is far enough from the wire, $r_2 / (x - a) < 0.04$. For protein nanoparticles, the strong inequality $r_2 \ll a$ is met and, even at $a = 10^{-4}$ cm, $x = 1.2 \cdot a$, $r_2 = 4 \cdot 10^{-7}$ cm, the ratio of these times is much smaller than unity, $\tau_r / \tau_f \approx 10^{-1}$. For a micrometer bioparticle, the condition $\tau_r / \tau_f \ll 1$ is met at $x > 10^{-2}$ cm.

Integrating Eq.(16) at the fixed particle coordinate x , we get the estimate of the time of its complete turn from the vertical ($\theta = \pi/2$) to the almost horizontal ($\theta = (\pi - 0.1)$ rad) position,

$$\tau_r = 4.5 \frac{\eta kT (r_1 + r_2) (4r_1^2 - r_1 r_2 + 4r_2^2) x^5}{N G^2 \mu_B^2 M_s (2\pi M_s a^2 + H_0 x^2) a^2 r_2}.$$

3.2. We numerically estimate the time of total orientation of the bioparticle for the protein molecule under the typical experimental conditions: $H_0 = 300$ Oe, $M_s = 1700$ Gs [8], $G = 5.6$, $\eta = 10^{-2}$ g · cm⁻¹ s⁻¹, $T = 293$ K, $N = 48$ (ferritin, see [10]) and $N = 200$ ions (a cluster, consisting of several ferritin molecules). Let the iron wire be thin, $a = 10^{-4}$ cm, and the size of the iron free region of the molecule be $r_2 = 4 \cdot 10^{-7}$ cm. Figures 3 and 4 display the dependences of the particle orientation time Eq.(19) on the ratio of model sphere radii (Fig.3 at $x = 1.5 a$) and on the distance to the

wire (Fig.4 at $r_1/r_2 \rightarrow 0$). Figure 3 shows that time of the particle orientation is decreased in the magnetic field at $r_1/r_2 \rightarrow 0$, that is, as the nonuniformity of the distribution of magnetic incorporations increases. In this case, the particle structure tends to the limiting value: the protein molecule with point (concentrated to the maximum) localization of Fe-iron-ion incorporations. In this structure, the torque moment is a maximum, and the surrounded fluid flows with the least resistance. It is the structure of the incorporations that is optimal for molecule orientation in the magnetic field. The typical times (calculated neglecting rotational diffusion) of the complete turn of a molecule are shown in Fig.4. However, we note that a turn of each molecule of the ensemble at an angle much smaller than $\Delta\theta \approx \pi/2$ in Eq.(19) is sufficient for anisotropy (such as optical) effects to be manifested. Before turning on the magnetic field, the molecule orientations are uniformly distributed over all angles. Hence, no anisotropy-related effects can be observed. When the field is "on", molecules begin to orient themselves along it. However, the orientation is counteracted by rotational diffusion taking place due to thermal motions of surrounding liquid molecules. The competition of the two processes creates a statistical equilibrium anisotropic orientational distribution of molecules. Below we will show that field-induced changes in the orientational distribution are small in our case. The average change in the orientation angle of a separate molecule is much less than $\pi/2$, and turn time is much shorter than τ_r . In this case, the settling time of the anisotropic distribution after turning on the magnetic field is controlled by the rotational diffusion time (see Sec.3.3), rather than by the magnetic field. The complete turn time τ_r calculated above is an upper estimate of the settling time, exceeding the true value by a few orders of magnitude in our case.

3.3. In micrometer bioparticles, the number N of magnetic Fe ions can be orders of magnitude larger if the first sphere in the model of Fig.2 is made from a superparamagnetic biomaterial with rather high magnetic permeability μ . The above-mentioned relations and estimates may also be applied to similar microparticles at a given magnetic permeability if the number N of Fe ions is written in terms of the magnetic permeability and the size of the magnetized region. The approximate equation for N may be derived by comparing Eq.(3) with the equation $\mathbf{m} \approx (\mu - 1)r_1^3 \mathbf{H}/3$ ($\mu - 1 \ll 1$) for the magnetic moment induced in the first (paramagnetic) sphere,

$$N = \frac{kT(\mu - 1)}{(G\mu_B)^2} r_1^3.$$

In this case, the equations for magnetic force Eq.(5) and complete turn time Eq.(19) of the bioparticle yield

$$\mathbf{F}_m = \frac{4\pi(\mu - 1)}{3} r_1^3 \cdot \nabla w,$$

$$\tau_r = 4.5 \frac{\eta(r_1 + r_2)(4r_1^2 - r_1 r_2 + 4r_2^2)x^5}{(\mu - 1)M_s \left(2\pi M_s a^2 + H_0 x^2\right) a^2 r_1^3 r_2}.$$

As will be shown below, the reverse situation is typical for micrometer bioparticles: the orientational distribution can be strongly anisotropic, and the distribution settling time corresponds to the dynamic estimate Eq.(21).

4. Orientation angle distribution of iron containing bioparticles. Anisotropy settling and disturbance times

4.1. To determine the orientational distribution of iron containing bioparticles in the field of a magnetized wire, we consider an ensemble of these particles. We utilized the optimum model with $r_1 \ll r_2$, $r_2 \approx r_{21} \approx r_p$, defined above. This simple model, with a quasipoint localization of Fe ions, makes it possible to discard the above restrictions imposed to the particle position and orientation. Furthermore, for this model we can immediately use the results of the theory of rotational Brownian motion of spherical particles. We consider an arbitrary position of bioparticles. The sphere center coordinates $\{x, y, z\}$ are bounded only by the condition $\tau_r / \tau_f \ll 1$ (see Eq.18), when these coordinates may be considered approximately constant for each particle. The bioparticle orientation is also supposed to be arbitrary and is now described by two angles $\{\theta, \varphi\}$. These are the angular coordinates of the vector \mathbf{r}_{21} from the sphere center to the point of magnetic incorporation localization in the spherical frame of reference, whose preferred axis is parallel to the wire magnetization vector \mathbf{M}_s (that is, the axis x of the initial Cartesian system, see Fig.2).

The relation $r_1 \sim r_2$ is typical for micrometer bioparticles; therefore, the results obtained within the model of quasi-point incorporation localization require correction. This is mostly related to the correction of the mechanical moment of the liquid rotation of the resistance (see Eq.12)). Nevertheless, this model yields simple relations, which should in turn yield accurate (at least in the order of magnitude) estimates at $r_1 \sim r_2$ as well.

The model particle is subject to only two concentrated forces: magnetic Eq.(5) and Stokes Eq.(11). As follows from the equilibrium condition, they are equal in magnitude and opposite in direction. The magnetic and the Stokes forces are applied at the point of magnetic incorporation at the sphere surface and at the sphere center, respectively. The bioparticle rotation maintains the mechanical moment of this pair of forces, and this moment is equal to the vector product

$$\mathbf{K}_m = [\mathbf{r}_{21} \times \mathbf{F}_m].$$

Equation (22) is similar to the expression of a mechanical moment rotating a dipole in a uniform field. Hence, taking into account Eq.(1), the potential energy for the iron containing bioparticle is given by

$$U = -(\mathbf{r}_{21} \mathbf{F}_m) = -(\mathbf{m} \nabla)(\mathbf{H}_s \mathbf{r}_{21}).$$

In contrast to the energy of a dipole placed into a uniform field, the effective energy of the orientation of a magnetic particle Eq.(23) is defined by the spatial derivative of the magnetic field with respect to the direction of the induced magnetic moment of incorporations. In the paramagnetic model of incorporations, Eq.(3), with a given N , the orientation energy is written as

$$U = -\frac{4\pi N G^2 \mu_B^2}{3kT} (r_{21} \nabla w)$$

To express this in terms of the magnetic permeability (μ_B) and the size of the magnetized region (\mathbf{r}_1), we use equation 20 to obtain:

$$U = -\frac{4\pi(\mu-1)r_1^3}{3}(r_{21}\nabla w) \quad (24a)$$

For the scheme for inducing a high-gradient magnetic field (see Fig.1), the calculation of orientation energy Eqs.(24, 24a) yields

$$U = -\frac{4\pi N G^2 \mu_B^2 M_s r_p a^2}{3kT(x^2 + y^2)^3} \times \\ \times \left\{ \left[2\pi M_s a^2 + H_0(x^2 - 3y^2) \right] \cdot x \cos\theta + \left[2\pi M_s a^2 + H_0(3x^2 - y^2) \right] \cdot y \sin\theta \cos\phi \right\}.$$

Comparison of Eqs.(24, 24a) to the energy of a dipole oriented in the uniform field [11,12] shows that the effective dipole moment is given by

$$\mu_{\text{eff}} = \frac{N G^2 \mu_B^2 H}{3kT} \cdot \frac{\mathbf{r}_{21}}{r_{21}} = \frac{(\mu-1)r_1^3 H}{3} \cdot \frac{\mathbf{r}_{21}}{r_{21}},$$

if the normalized gradient of the energy density $\frac{4\pi r_{21}}{H} \nabla w$ acts as the effective field.

4.2. The balance between the directed rotation of bioparticles under the action of moments (Eq.22 and 12), as well as rotational Brownian motion, results in an equilibrium Boltzmann orientational distribution of these particles (see, for example, [12,13]),

$$\Phi(\theta, \phi) = \frac{\exp\left[-\frac{U}{kT}\right]}{\int_0^\pi \left(\int_0^{2\pi} \exp\left[-\frac{U}{kT}\right] d\phi \right) \sin(\theta) d\theta}.$$

The transition to the Boltzmann distribution Eq.(27) from the uniform distribution

$$\Phi_0(\theta, \phi) = \frac{1}{4\pi}$$

that existed before turning on the field is given by the rotational diffusion equation [11,12]:

$$\frac{\partial \Phi}{\partial t} = D \frac{\partial}{\partial s} \left[(1-s^2) \cdot \left(\frac{\partial \Phi}{\partial s} + \beta \Phi \right) \right],$$

where $s = \frac{(\mathbf{r}_{21} \nabla w)}{|\mathbf{r}_{21}| \cdot |\nabla w|}$ is the cosine of the angle between \mathbf{r}_{21} and the energy density gradient ∇w

. The approximate equation $s \approx \cos\theta \cos\psi + \sin\theta \cos\phi \cos\psi$ is valid near the wire, where

$H_0 \ll H_s$, (this region is appropriate for molecules with $r_p \ll a$). The rotational diffusivity D is given by

$$D = \frac{kT}{8\pi r_p^3 \eta}$$

The parameter β defines the steady-state anisotropy degree,

$$\beta = \frac{U_m}{kT},$$

where U_m is the maximum orientation energy achieved at $s = -1$.

For nanoparticles (molecules), the values of β are small at reasonable temperatures. For example, estimation for the layout of Fig.1 at the parameters of Sec.3.2 yields

$$\beta \leq \frac{4\pi N G^2 \mu_B^2 M_s (2\pi M_s + H_0) r_p}{3k^2 T^2 a} < 2 \cdot 10^{-4}.$$

In the case of micrometer bioparticles, the parameter β can be much larger than unity. We estimate β for small values of the magnetic field and its gradient, $H = 300$ Oe, $|\nabla H| = 200$ Oe/cm. It is easy to get these values: they take place, for example, in the layout of Fig.1 at a rather long distance from the wire, $x = 10^{-2}$ cm, at $a = 10^{-4}$ cm, $H_0 = 300$ Oe, $M_s = 1700$ Gs. The condition $\tau_r / \tau_f \ll 1$ (see Eq.(18)) is already met at this distance from the wire. For bioparticles with sizes $r_1 = r_2 = 1.4 \cdot 10^{-4}$ cm, containing a superparamagnetic incorporation ($\mu = 1.1$), we find $\beta \approx 20$. In this case, distribution Eq.(27) is close to the Dirac delta function.

To determine the settling time of the equilibrium distribution, we consider, proceeding from the above estimates, the solution of Eq.(29) in two extreme cases, $\beta \ll 1$ and $\beta \gg 1$, which are important for biomolecules and micrometer particles, respectively.

4.2.1. In the former case, we find the solution to Eq.(29) by expanding the distribution function Φ into the series with respect to small β ,

$$\Phi = \frac{1}{4\pi} \left[1 + \beta s (1 - e^{-2D t}) + \frac{\beta^2 (3s^2 - 1)}{12} (2 - 3e^{-2D t} + e^{-6D t}) \right].$$

This equation yields the estimate of the settling time τ_Φ of the equilibrium distribution function Eq.(27) after turning on the magnetic field,

$$\tau_\Phi = \frac{1}{2D} = \frac{4\pi\eta r_p^3}{kT}.$$

With $\beta \ll 1$, the settling time depends only on the biomolecule size, liquid viscosity, and temperature. For the scheme of Fig.1, at the field and biomolecule parameters considered in Sec.3.2, we have

$$\tau_{\Phi} = 2 \cdot 10^{-7} \text{ s} ,$$

which is by a few orders of magnitude less than the time, τ_r , in the dynamic model given by Eq.(19), because the small turn angle (of the order of β) in Eq.(27) in comparison with Eq.(19). An isotropic distribution Eq.(28) after turning off the field is restored on the same time scale Eq.(34) and Eq.(35).

4.2.2. In the second case, it follows from $\beta \gg 1$ that $\frac{\partial \ln(\Phi)}{\partial s} \ll \beta$; that is, the diffusion flow in Eq.(29) is weak in comparison to the drift situation. In this case, Eq.(29) is reduced to the equation

$$\frac{\partial \Phi}{\partial t} = D \frac{\partial}{\partial s} \left[(1 - s^2) \cdot \beta \Phi \right],$$

which has an analytical solution meeting the initial condition $\Phi(\theta, \varphi) \Big|_{t=0} = \frac{1}{4\pi}$:

$$\Phi = \frac{1}{4\pi} \left[\cosh(\beta D t) - s \cdot \sinh(\beta D t) \right]^2 .$$

Equation (37) yields the estimate of the settling time τ_{Φ} of the equilibrium anisotropic distribution after turning on the magnetic field,

$$\tau_{\Phi} = \frac{1}{\beta D} = \frac{6\eta r_p^2}{(\mu - 1)r_1^3 |\nabla w|} .$$

Let us compare Eq.38 to turning time Eq.21 for the model of Fig.1. Substituting Eqs.6, 8, and 9 into Eq.38 and putting $r_1 \ll r_2 \approx r_p$ in Eq.21, we find that the time τ_r differs from τ_{Φ} only by a numerical coefficient of about three. This difference is actually caused only by the different definitions of these times: τ_{Φ} is the characteristic scale of the orientation time variation and τ_r is the time of the particle to complete a turn to an almost horizontal position ($\theta = (\pi - 0.1)$ rad). Hence, the dynamic orientation mode is achieved at $\beta \gg 1$, which is described by Eqs.11 through 16. This case is important for rather large (micrometer) bioparticles. In distribution function Eq.(29), the dynamic mode corresponds to a negligible diffusive flow.

In the case where $\beta \gg 1$, after turning off the field, the isotropic distribution Eq.(28) is restored with a characteristic time $\tau_{\Phi, \text{off}}$, differing from that given by Eq.(38). The isotropic distribution is restored according to the rotational diffusion mechanism; independently of β , the restoring time $\tau_{\Phi, \text{off}}$ is given by

$$\tau_{\Phi, \text{off}} = \frac{1}{2D} = \frac{4\pi\eta r_p^3}{kT} .$$

When $\beta \gg 1$, the time $\tau_{\Phi, \text{off}}$, is longer than the anisotropy settling time Eq.(38) by approximately a factor of $\beta/2$. Thus, the disorder at $\beta \gg 1$ for rather large particles and strong magnetic fields is restored slower than the particle orientation.

We estimate the characteristic times for micrometer bioparticles with the parameters of Sec.4.2: $H = 300 \text{ Oe}$, $|\nabla H| = 200 \text{ Oe/cm}$, $\mu = 1.1$, $r_1 = r_2 = 1.4 \cdot 10^{-4} \text{ cm}$. In this case, the parameter β is about 20. At this value, the steady-state orientational distribution is strongly anisotropic. Almost all the bioparticles are oriented antiparallel to the gradient ∇w . For a nonuniform field, according to the layout of Fig.1, this means that almost all the bioparticles oriented so that the paramagnetic incorporations are closed to the wire while the non paramagnetic portion is further away. In this case, the characteristic anisotropy settling and disturbance times are $\tau_{\Phi} \approx \frac{1}{3} \tau_r \approx 1 \text{ s}$ and $\tau_{\Phi, \text{off}} \approx 10 \text{ s}$, respectively.

5. Anisotropy effects in protein molecules, $\beta \ll 1$

The attainable anisotropy of the equilibrium distribution Eq.(27) is insignificant because of the rather small sizes of biomolecules Eq.(32). Let us consider the possibility to measure this anisotropy using the layout of Fig.1 with a nonuniform magnetic field.

The possible experimental methods for measuring the anisotropic orientational distribution of protein molecules can be classified into two groups.

5.1. The methods of one group are based on linear effects; the values observed are proportional to the cosine (averaged over distribution Eq.(27)) of the tilt angle θ of molecular axes to the magnetization vector \mathbf{M}_s (see Fig.1),

$$\langle \cos \theta \rangle = \int_0^{\pi} \left(\int_0^{2\pi} \Phi(\theta, \phi) \cos \theta \, d\phi \right) \sin \theta \, d\theta .$$

Using the smallness of anisotropy Eq.(32), and expanding the exponent in Eq.(27) into a series with respect to small parameter $\beta = 1$, from Eq.(40) we arrive at

$$\langle \cos \theta \rangle = - \frac{4\pi N G^2 \mu_B^2 M_s r_p a^2 x \left[2\pi M_s a^2 + H_0 (x^2 - 3y^2) \right]}{9 k^2 T^2 (x^2 + y^2)^3} .$$

The dependence of $\langle \cos \theta \rangle$ on the arrangement of protein molecules with respect to the magnetized wire is shown in Fig.5. The calculation was carried out for the same parameters as found in Sec.3.2: $r_p = 4 \cdot 10^{-7} \text{ cm}$, $T = 293 \text{ K}$, $H_0 = 300 \text{ Oe}$, $a = 10^{-4} \text{ cm}$, $M_s = 1700 \text{ Gs}$. The average cosine of the orientation angle strongly abates as receding from the wire even at a distance of the order of its radius. As expected, the maximum anisotropy should be observed for molecules arranged in the vicinity of the wire surface near plane zx : in this case, $\langle \cos \theta \rangle$ is estimated as

$$|\langle \cos\theta \rangle|_{\max} \approx \frac{8\pi^2 N G^2 \mu_B^2 M_s^2 r_p}{9k^2 T^2 a}.$$

One can see in Fig.5 that molecules arranged on each side of plane yz are oriented in opposite direction because the $\langle \cos\theta \rangle$ sign reverses. Hence, the total linear effect over all the molecules vanishes. To observe the anisotropy using linear effects, one should separate the halfspace into $x < 0$ or $x > 0$. When optical effects are used to measure the anisotropy, an observation position can be easily achieved by exposing a space region on one side of the wire to a focused laser beam. To determine the quantitative characteristic of the total linear effect of the anisotropy measurement, we integrate $\langle \cos\theta \rangle$ over all possible molecule coordinates meeting the condition $x < 0$, and multiply it by the iron containing molecule density n_p . The physical meaning of this integral characteristic is the effective number N_1 of molecules completely oriented in the halfspace. The problem is homogeneous with respect to coordinate z , and N_1 is interpreted as the specific (calculated per wire unit length) one. As a result we arrive at

$$N_1 = n_p \iint_{\substack{x^2+y^2 > a^2 \\ x < 0}} \langle \cos\theta \rangle dx dy = \frac{8\pi N G^2 \mu_B^2 M_s (2\pi M_s - H_0) r_p a}{27k^2 T^2} n_p.$$

The integral anisotropy characteristic Eq.(43) increases with the wire radius, a . Furthermore, the above-mentioned spatial selection should be provided for the linear measurement of anisotropy. In this case, the efficiency of a spatial grid consisting of many parallel magnetized wires is not high. It is a better practice to employ a single sufficiently thick wire, or a few wires, maintaining spatial selection for each. If the density of iron containing molecules is $n_p = 4 \cdot 10^{16} \text{ cm}^{-3}$ and the wire radius is $a = 10^{-2} - 10^{-1} \text{ cm}$ under the above-mentioned experimental conditions, the effective number of completely oriented particles is $N_1 \approx (2 \cdot 10^4 - 2 \cdot 10^5) \text{ cm}^{-1}$ for $N=4$ (hemoglobin), $N_1 \approx (2 \cdot 10^5 - 2 \cdot 10^6) \text{ cm}^{-1}$ for $N=48$ (ferritin), and $N_1 \approx (10^6 - 10^7) \text{ cm}^{-1}$ for $N=200$ (probable candidate molecule). These values are quite measurable.

5.2. If the measurement of the anisotropic orientation of molecules is based on nonlinear effects, the values observed are proportional to the quadratic characteristic $\cos^2\theta - 1/3$ averaged over distribution Eq.(27),

$$\left\langle \cos^2(\theta) - \frac{1}{3} \right\rangle = \int_0^\pi \left(\int_0^{2\pi} \Phi(\theta, \phi) \cdot \cos^2(\theta) \cdot d\phi \right) \sin(\theta) d\theta - \frac{1}{3}.$$

To calculate integral Eq.(44), condition Eq.(32) is also used; as a result we arrive at

$$\left\langle \cos^2 \theta - \frac{1}{3} \right\rangle = \frac{1}{5} \left[\frac{4\pi N G^2 \mu_B^2 M_s r_p a^2}{9 k^2 T^2 (x^2 + y^2)^3} \right]^2 \times$$

$$\times \left[4\pi^2 M_s^2 a^4 (2x^2 - y^2) + 4\pi M_s H_0 a^2 (2x^4 - 9x^2 y^2 + y^4) + H_0^2 (2x^6 - 21x^4 y^2 + 24x^2 y^4 - y^6) \right]$$

The dependence of $\left\langle \cos^2 \theta - \frac{1}{3} \right\rangle$ on the molecule arrangement with respect to the magnetized wire is shown in Fig.6. The calculation was carried out with the parameter values of Fig.5. The orientation degree strongly decreases with the distance from the wire and is maximum for molecules arranged in the vicinity of the wire surface near plane zx ; the maximum of this value is estimated by the equation

$$\left[\left\langle \cos^2 \theta \right\rangle - \frac{1}{3} \right]_{\max} \approx \frac{2}{5} \left[\frac{8\pi^2 N G^2 \mu_B^2 M_s^2 r_p}{9 k^2 T^2 a} \right]^2.$$

Figure 6 shows that the total quadratic effect over all the molecules does not vanish. To determine the quantitative characteristic of this effect in the measurement of the anisotropy induced by a wire, we integrate $\left\langle \cos^2 \theta \right\rangle - \frac{1}{3}$ over the whole space except for the wire volume, multiply it by the iron containing molecule density n_p and by a factor of $3/2$. The physical meaning of this integral characteristic N_{nl} is the effective number of completely oriented molecules for the measurement of distribution anisotropy using nonlinear effects. The problem is homogeneous over the coordinate z ; therefore, we do not integrate over z . The parameter N_{nl} is interpreted as the specific one, calculated per unit length of the wire,

$$N_{nl} = \frac{3}{2} n_p \iint_{x^2+y^2>a^2} \left\langle \cos^2 \theta - \frac{1}{3} \right\rangle dx dy = \frac{2}{135} \frac{\pi^3 N^2 G^4 \mu_B^4 M_s^2 r_p^2 (2\pi^2 M_s^2 + H_0^2)}{k^4 T^4} n_p.$$

Integral characteristic Eq.(47) is independent of the wire radius. For estimations, we put $r_p = 4 \cdot 10^{-7}$ cm, $T = 293$ K, $M_s = 1700$ Gs, and $H_0 = (300-3000)$ Oe. Then, at a density of iron containing molecules $n_p = (10^{16}-10^{17})$ cm⁻³, we have $N_{nl} \approx (5 \cdot 10^{-6}-5 \cdot 10^{-5})$ cm⁻¹ for $N=4$ (hemoglobin), $N_{nl} \approx (10^{-3}-10^{-2})$ cm⁻¹ for $N=48$ (ferritin), and $N_{nl} \approx (10^{-2}-10^{-1})$ cm⁻¹ for $N=200$ (probable candidate molecule).

In a nonlinear measurement, the anisotropy integral effect may be significantly enhanced by using a structure of many parallel magnetized wires. The effect of a solitary wire is independent of its thickness a (see Eq.47); therefore, wires as thin as possible should be used in the structure, which would allow denser arrangement. This is because the summation of the effects from each wire is effective when neighbors do not strongly decrease the gradient of the field induced by a solitary wire. Moreover, the size of the molecule orientation region (at $r_p \ll a$) is of the order of a near a solitary wire. Hence, the allowed distance between the wires is shortened as their radius decreases. A preliminary

analysis shows that the distance d_y between the wires should be long ($d_y > 10 \cdot a$) in the direction perpendicular to the magnetizing field. This is because the field of the neighbors arranged in this direction is directed oppositely to the eigenfield of each magnetized wire (see Eq.10). Wires may be more densely arranged in the direction parallel to the magnetizing field (along the x axis). According to preliminary estimate, the optimal distance between the axes of neighboring wires is $(3-4) \cdot a$ in this direction. Due to an increase in the total number of molecules appearing in a sufficiently strong nonuniform field, the gain multiplicity of the integral effect of the anisotropy measurement using this multiwire grid structure can be of the order of the total number of wires. Therefore, the above estimate of the effective number of completely turned molecules can be increased by a few orders of magnitude. For example, in the case of optimal filling of a 1cm^3 volume with wires having radius $a = 10^{-4}\text{cm}$, where volumes extended along the axis z are more advantageous in practice, because they require fewer wires, the effective number of oriented molecules in this volume can reach 10^4 for ferritin ($N=48$) and 10^5 for a ferritin cluster ($N>100$). It should be emphasized that, according to Eqs.34 and 35, the characteristic orientation of time does not exceed 10^{-6}s if the molecule diameter is smaller than 10^{-6}cm .

6. Conclusion

The necessary conditions of the biomolecule orientation mechanism proposed are a nonuniform external magnetic field and a nonuniform distribution of Fe ions in the biomolecule. This mechanism is universally valid in the presence of these nonuniformities and can vary only quantitatively. We emphasize that our calculation yields only a lower estimate of the orientation effect, because two other mechanisms can also manifest themselves: first, the finite rigidity of the Fe-ion magnetic moment bonds with the neighboring atoms and second, ferromagnetic ordering. Additional mechanisms can significantly enhance the orientation effect. Analysis and estimation of the prerequisites of these mechanisms is a subject of further investigation.

The effect is enhanced by a few orders of magnitude by a grid structure consisting of many parallel thin magnetized wires. The wires may be more densely arranged along the field than across the field. Optimization of the parameters of the grid structure is also a promising direction, especially for biomolecules whose size is significantly smaller than the wire diameter.

The conditions of realization and observation of the orientation mechanism, as well as the prospects of its application, may be radically improved by passing from molecules to micrometer bioparticles. Simple bioparticles composed of two spherical components, one of which reveals superparamagnetic properties [5], were shown to be completely oriented in reasonable magnetic fields within a time of the order of a second. The orientation time can be decreased by using complicated (for example, unidirectionally extended) structures, stronger magnetic fields and artificially constructed superparamagnetics.

The authors are thankful to A.V. Krasnoslobodtsev for fruitful discussions.

This project has been funded in whole or in part with Federal funds from the National Cancer Institute, National Institutes of Health, under Contract numbers N01-C0-56000 and N01-C0-12400, by RFBR Projects 00-15-96636 and 02-02-16184, as well as the Integration of Russian Science and Higher Education for 2002-2006 Federal Program (Contract No.04-10).

References

1. Biophysical Effect of Steady Magnetic Fields. Proc. Workshop hes Houches. Berlin: Springer, 1987.
2. Shalygin A.N and Krotov K.A. Usp. Fiz. Nauk 1990, 160(7), 83 (Sov. Phys. Usp.).
3. Shalygin A.N. and Krotov K.A. Biofizika 1988, 33, 529.
4. Wernsdorfer W, Aliaga-Alcalde N, Hendrickson DN, Christou G. Nature 2002, 416, 406.
5. Landau L.D. and Lifshitz E.M. Electrodynamics of Continuous Media. Reading, Mass.: Addison--Wesley.
6. Ziman J.M. Principles of the Theory of Solids. Cambridge: Cambridge Univ., 1972.
7. Haurowitz F. The Chemistry and Function of Proteins. N.Y.: Academic, 1963.
8. Tables of Physical Values. Handbook. Ed. I.K. Kikoin. Moscow: Atomizdat, 1976 [in Russian].
9. Landau L.D. and Lifshitz E.M. Hydrodynamics. Reading, Mass.: Addison--Wesley.
10. Hempstead P.D., Yewdall S.J., et al. J. Mol. Biol. 1997, 268, 424.
11. Landau L.D. and Lifshitz E.M. Field Theory. Reading, Mass.: Addison--Wesley.
12. Vuks M.K. Electrical and Optical Properties of Molecules and Condensed Media. Leningrad: LGU, 1984 [in Russian].
13. Debye P. and Zakk G. Theory of the Electrical Properties of Molecules. Moscow: Gostekhizdat, 1936 [in Russian].

Figure captions

Fig.1. Scheme of induction of a high-gradient magnetic field.

Fig.2. Model of an inhomogeneous bioparticle with paramagnetic incorporations; the forces acting upon a bioparticle moving in a liquid.

Fig.3. Dependence of the time of a complete turn of the molecule on the ratio of model sphere radii: r_1 is the radius of the iron containing sphere, $r_2 = 4 \cdot 10^{-7}$ cm is the radius of the sphere without incorporations. The dependence was calculated at $a = 10^{-4}$ cm, $H_0 = 300$ Oe, $M_s = 1700$ Gs, and $G = 5.6$ for $N = 48$ (a), and $N = 200$ (b); the distance to the wire is $x = 1.5 \cdot a$.

Fig.4. Dependence of the time of a complete turn of the molecule on the distance to the magnetized wire at $r_1 = 0$. The values of other parameters are the same as in Fig.3.

Fig.5. Average cosine $\langle \cos \theta \rangle$ of the orientation angle of protein molecules versus the normalized coordinates (x/a and y/a) defining the molecule position with respect to the magnetized wire. The values of the parameters are the same as in Fig.4. Axis x is parallel to the wire magnetization vector.

Fig.6. Coordinate dependence of the orientational ordering degree $\left\langle \cos^2 \theta - \frac{1}{3} \right\rangle$ of protein molecules. The values of the parameters are the same as in Fig.4.

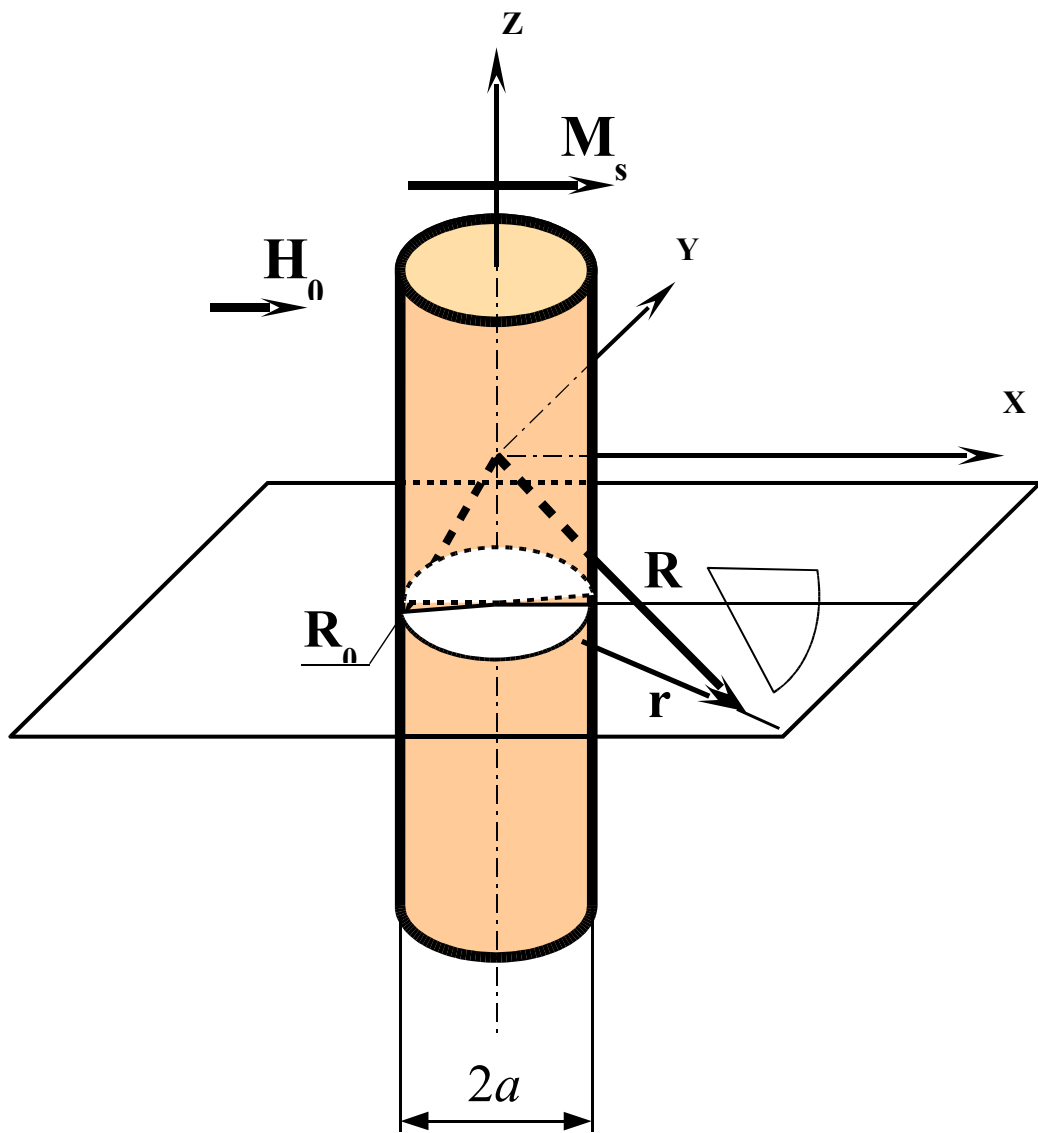


Fig. 1

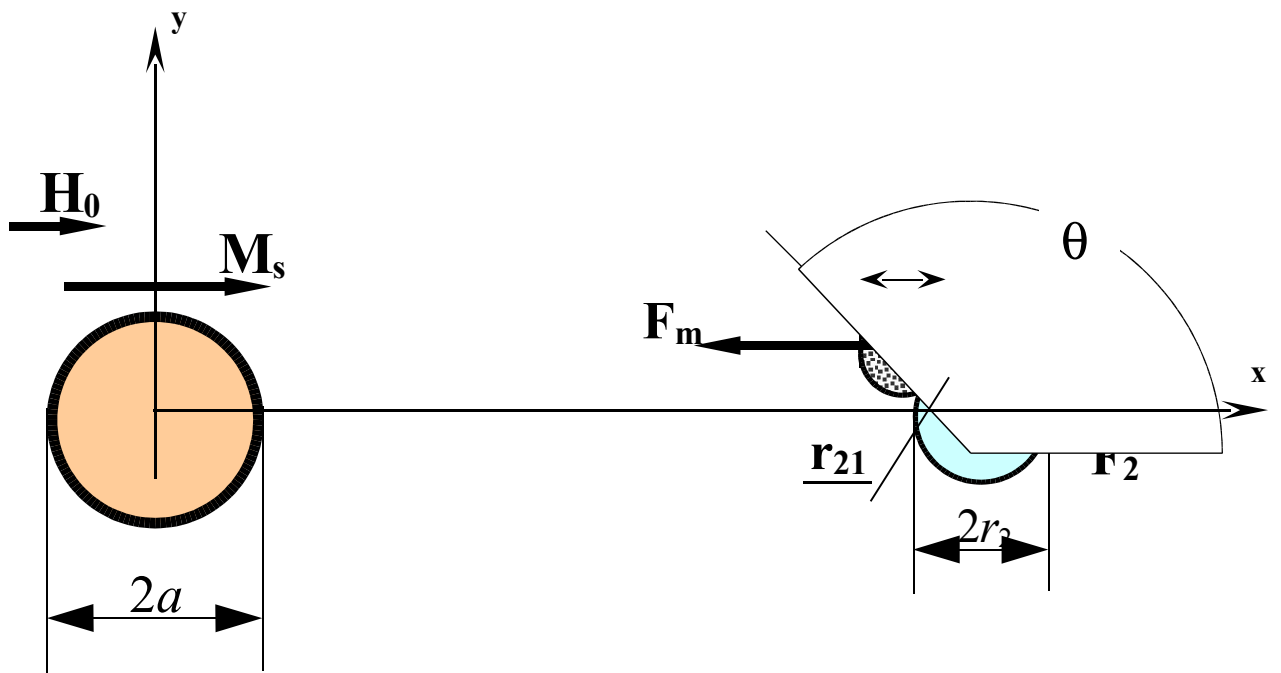


Fig. 2

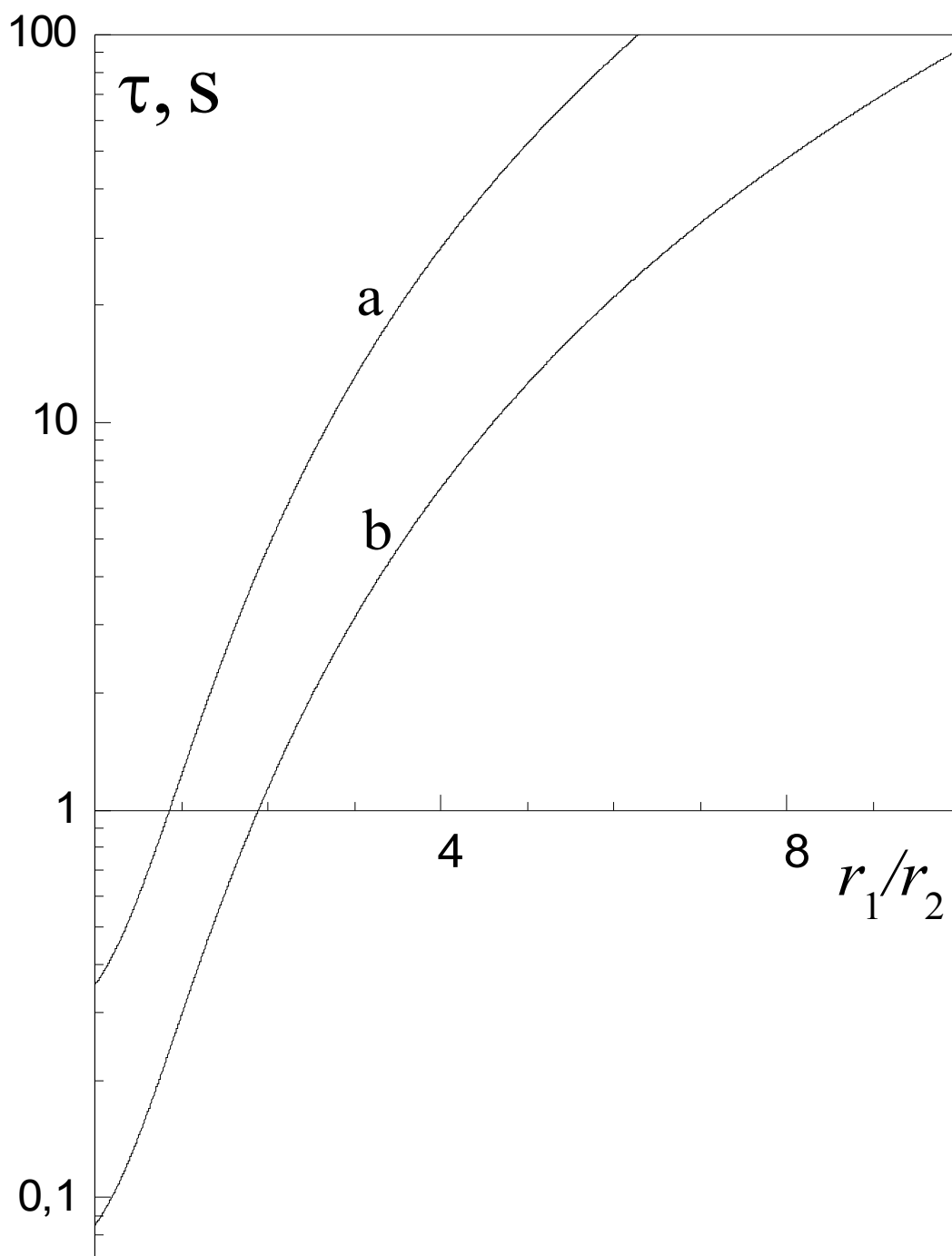


Fig. 3

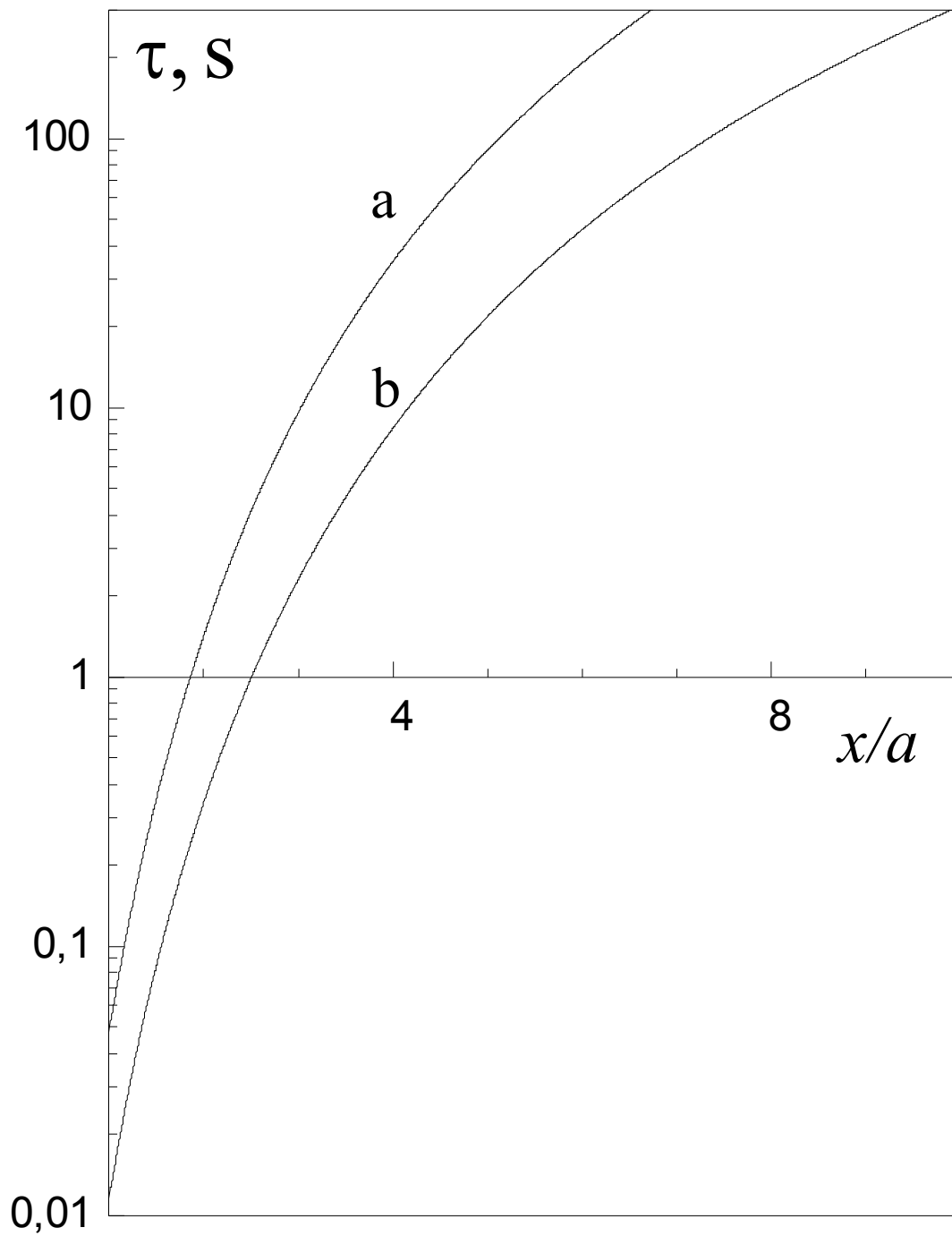


Fig. 4

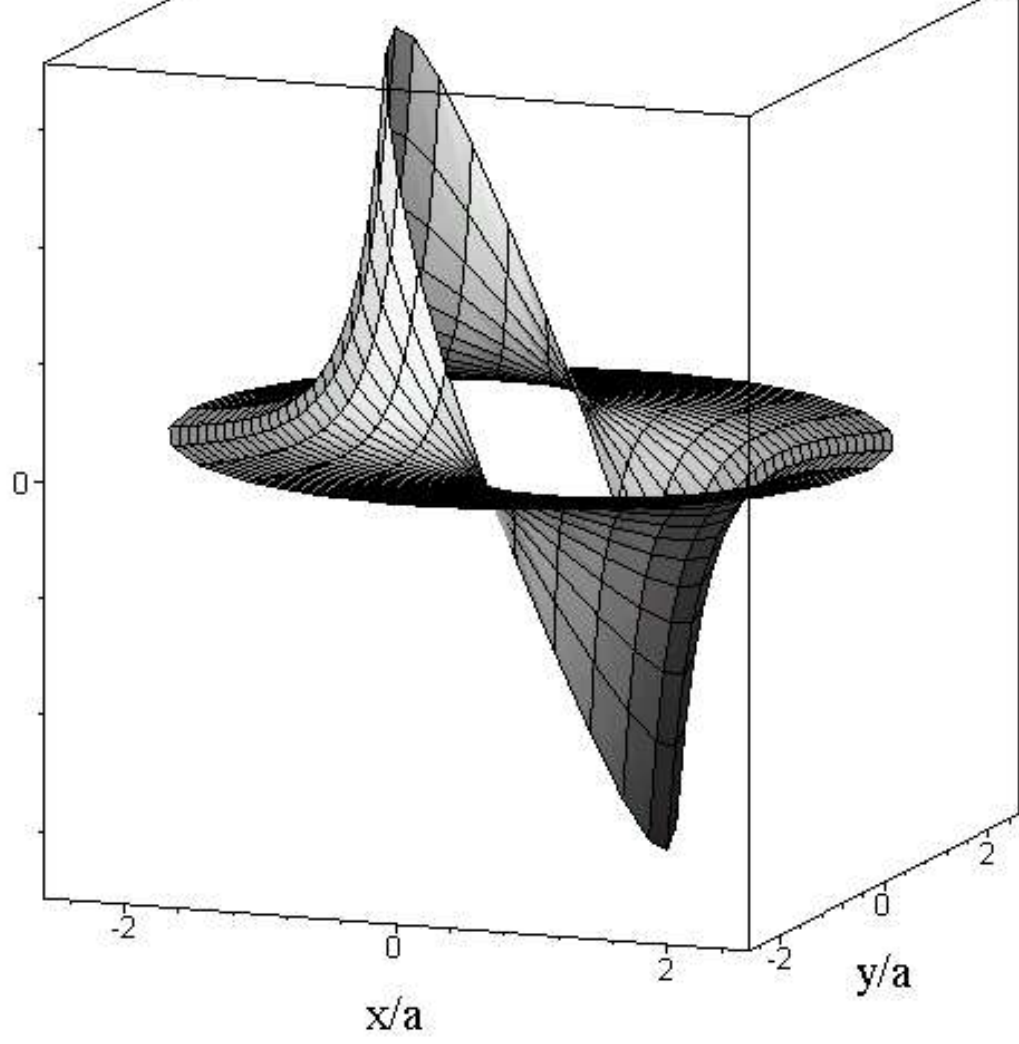


Fig. 5

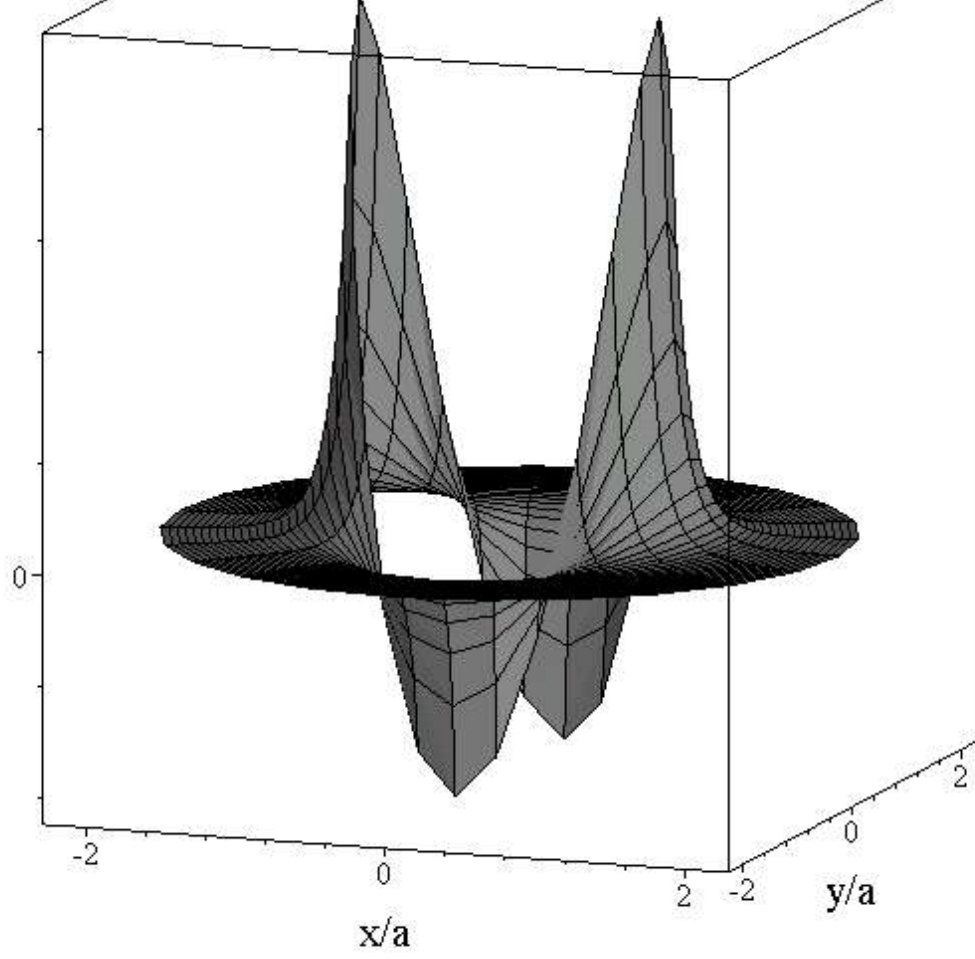


Fig. 6